Journal of Alloys and Compounds 505 (2010) 640–644

Contents lists available at ScienceDirect

Journal of Alloys and Compounds

journal homepage: www.elsevier.com/locate/jallcom

Fluorine-free sol–gel preparation of $YBa_2Cu_3O_{7-x}$ superconducting films by a direct annealing process

Y. Chen*, F. Yan, G. Zhao, G. Qu, L. Lei

Department of Materials Physics & Chemistry, Xi'an University of Technology, Xi'an 710048, PR China

ARTICLE INFO

Article history:
Received 29 March 2010
Received in revised form 12 June 2010
Accepted 14 June 2010
Available online 25 June 2010

Keywords:
High Tc superconductor
Thin film
Chemical synthesis
Sol–gel process

ABSTRACT

Using yttrium, barium and copper acetates as starting materials, fluorine-free YBCO precursor solution is prepared by the chemical complexation approach with diethylenetriamine, lactic acid, and α-methacrylic acid as complexing agents. Using the stable precursor solution, YBCO gel films are coated on $LaAlO_3$ substrate by the dip-coating method. Effect of different heat treatment processes on the phase evolution and final film properties are examined. Results indicate that, either in a dry or in a humidified atmosphere, it is difficult to obtain high-performance YBCO films by a traditional pyrolysis–annealing process, due to the formation of stable $BaCO_3$ phase during the pyrolysis process. On the contrary, using the fluorine-free precursor solution, epitaxial YBCO films with high Tc (>94 K) and Jc (>1 MA/cm^2) can be obtained using a direct annealing process without pyrolysis process.

1. Introduction

Chemical solution deposition (CSD), including the sol–gel process and metal–organic deposition (MOD) method, holds great potential of producing large-scale, biaxially-textured $YBa_2Cu_3O_{7-x}$ (YBCO) superconducting films. According to the solution compositions, CSD methods for preparation of YBCO films can be generally divided into two categories: the fluorine-free routes and the fluorinated routes.

The fluorinated routes using trifluoroacetates (TFA) as precursors have attracted much interest due to its high reproducibility in fabrication of high-quality YBCO films [1,2]. Today, process optimization has made the superconducting coated conductors derived from solution routes almost be commercialized [3–7]. However, the conventional TFA-MOD process using full metal–TFA salts in the precursor solution (All-TFA solution) generates a large amount of HF gas during the pyrolysis step. As a result, a long processing time and special gas flow are required to fabricate large-area crack-free precursor films, while the thickness of precursor films is limited to low values after single coating and pyrolysis [8]. In order to overcome these disadvantages, many efforts have been made to improve the process by reducing the fluorine content in the precursor solution [9–13].

For another, the fluorine-free sol–gel method has been developed and optimized for YBCO film preparation in the past decades. The fluorine-free sol–gel process is of great potential in the commercialization the of YBCO coated conductors due to its advantages, which includes: (1) no HF formed during the process, which is corrosive to the buffer layer or the metallic substrate; (2) much denser microstructure compared to TFA films; (3) no extra phases (such as BaF_2 in TFA approach), in addition to YBCO. Using the fluorine-free route, high-performance YBCO films, however, cannot be easily obtained as the fluorinated route. The underlying reason is thought to be that during the heat treatment process the stable $BaCO_3$ phase is easily formed, which blocks the formation of the YBCO phase and the transportation of superconducting current. To overcome this, metal acetylacetonates [14], metal naphthenates [15], metal trimethylacetates [16–18], and metal citrates [19], have been selected as precursors by some groups. And polymer-based YBCO precursor solution [20–23] has also been invented. All of these fluorine-free solution methods can be used to successfully prepare high-quality YBCO films.

So far, there have been few reports on the YBCO film preparation using cheap acetates as starting materials through the fluorine-free sol–gel method. In this paper, stable fluorine-free YBCO precursor solution is prepared using metal acetates as starting materials. To obtain phase-pure YBCO film with high superconductivity, a unique process, which is called one-step annealing process, is then put forward after detailed exploration of phase evolution during the heat treatment process. Using this method, high-performance

* Corresponding author. Tel.: +86 29 82312172.
E-mail address: chenyq@xaut.edu.cn (Y. Chen).

0925-8388/$ – see front matter © 2010 Elsevier B.V. All rights reserved.
doi:10.1016/j.jallcom.2010.06.098

YBCO superconducting films can be routinely prepared on $LaAlO_3$ (LAO) substrates in our laboratory.

2. Experimental

The traditional sol–gel method using alkoxides for preparation of YBCO precursor solution almost could not be realized since yttrium alkoxides are not available agents, and copper alkoxides show low solubility in organic solvents. In this experiment conducted, we select cheap inorganic acetates as starting materials. However, all the yttrium acetate, barium acetate, and copper acetate also show low solubility in organic solvents. This problem can only be solved by chemical modification or chemical complexation approach. In this experiment, three kinds of solutions are firstly prepared, which hereafter are named Y-OR solution, Ba-OR solution, and Cu-OR solution, respectively. To make Y-OR solution, yttrium acetate ($Y(OAc)_3$) is dissolved into 2-methoxyethanol (OREH) with the help of diethylenetriamine (DETA). To make Ba-OR solution, barium acetate ($Ba(OAc)_2$) is dissolved into OREH with the help of lactic acid. To make Cu-OR solution, copper acetate ($Cu(OAc)_2$) is dissolved into the mixture solution of α-methacrylic acid (HOAAα) and OREH.

The YBCO precursor solution is ready by mixing the Y-OR, Ba-OR, and Cu-OR solutions, with total metallic ion concentration controlled at about 0.5 mol/l and the molar ratio of metallic ions at Y:Ba:Cu = 1:2:3. Using the fluorine-free solution, YBCO gel films are dip-coated on single crystal (0 0 1)-oriented LAO substrate in a glove box, where the relative humidity is controlled below 30%R.H. The dip-coating rate is controlled at about 3–5 mm/s. The coated gel films are then heat treated in a furnace through two kinds of heat treatment processes: pyrolysis–annealing process and direct annealing process. Pyrolysis–annealing process: the coated gel films are dried at 200 °C for 10 min and pyrolyzed at 450 °C in air for 10 min. The coating–pyrolysis process is repeated for 2–3 times to build up the film thickness. After that, the pyrolyzed films are annealed at 780 °C in humidified N_2 with 1 vol.%O_2. Passing dry gas through the de-ionized water contained in a large flask, the humidified gas flow is obtained and then enters the furnace. After annealing at 780 °C for 2 h, the films are post-annealed at 450 °C in dry oxygen for 4 h. Direct annealing process: the coated gel films are inserted to the furnace, and heated from room temperature to 780 °C rapidly (20 °C/min) and then dwelled at 780 °C for 1.5 h in the humidified N_2/O_2 gas. This coating–annealing process can be repeated for several times to build up the film thickness. Finally, the films are post-annealed in dry oxygen for 4 h.

The FT-IR spectrometer is used to examine the organic groups in the solution and gel films. The film surface is observed under an Olympus-BX51 optical microscopy. A Philips X-ray diffractometer with Cu Kα radiation is used to carry out the texture investigations. A 7000S-type X-ray diffractometer (XRD) is used to perform the low-angle X-ray diffraction and theta–2theta diffraction on the films so as to detect the phases. Scanning electron microscopy (SEM) experiments are conducted on a JEM-6700F. No conductive coating is applied on the film surface. The film thickness was examined by a surface profilometer (Surfcorder SE3500 Kosaka). Measurements of resistance versus temperature are carried out down to liquid nitrogen temperature using a standard four-probe method. The obtained YBCO superconducting films are also patterned to be micro-bridge with the width of 250 μm. The *V–I* curve of the YBCO film is measured using the micro-bridge at 77 K so as to determine the Jc.

3. Results and discussion

3.1. Chemical reaction and complexation

The IR spectra are performed on the Y-OR solution, Ba-OR solution and Cu-OR solution. The results are as follows: (1) IR spectrum for Y-OR solution, ν, cm^{-1}: 1063.21 and 1125.38 (C–O–), 1203.82 (C–O–C), 2878.56 and 2930.13 (C–H), 1448.60 and 1569.87 (COO^-), 1598.14 and 3364.58 (N–H); (2) IR spectrum for Ba-OR solution, ν, cm^{-1}: 1070.72 and 1125.39 (C–O–), 1194.65 (C–O–C), 1456.16 (C–H), 1741.60 (C=O), 2931.60 (C–H), 3413.77 (–OH), 1455.24 and 1579.04 (COO^-); (3) IR spectrum for Cu-OR solution, ν, cm^{-1}: 1068.56 and 1126.35 (C–O), 1197.71 (C–O–C), 1456.16 (C–H), 1715.56 (C=O), 2881.45 and 2932.42 (C–H), 3411.84 (–OH), 1420.09 and 1551.53 (COO^-).

The yttrium acetate cannot be directly dissolved into the OREH solvent. However, after a long time stirring in OREH solvent mixed with bidentate type complexes (such as DETA), it gradually dissolves. This is due to the cleavage of inter-molecular coordination bonds and the partial substitution of acetate ligands in $Y(OAc)_3$ by DETA. The DETA has great ability to attract the proton (H^+), thus making the OREH become negatively charged ORE^- by the following Eq. (3-1).

$$\mathrm{DETA} + n\mathrm{OREH} = \mathrm{H}^{n+}\mathrm{DETA} + n\mathrm{ORE}^- \quad (3\text{-}1)$$

While the ORE^- can attract the Y^{3+}, and then open the bidentate type structure of OAc^- ligand, thus making the $Y(OAc)_3$ dissolved in OREH solvent. The reaction and the resulted yttrium complex can be expressed by formula (3-2) [24].

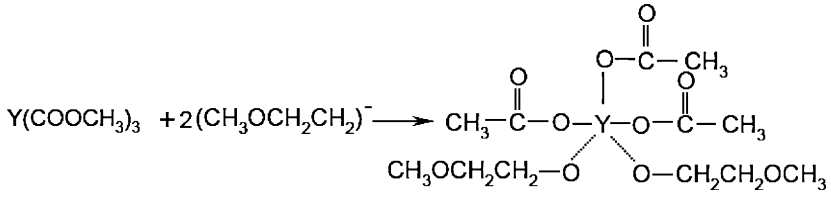

(3-2)

As to the Cu-OR solution, the complexing agent HOAAα can also make the $Cu(OAc)_2$ dissolved into the OREH. A series of complexing reactions take place in the solution, and the resulted complex can be expressed by formula (3-3) [25].

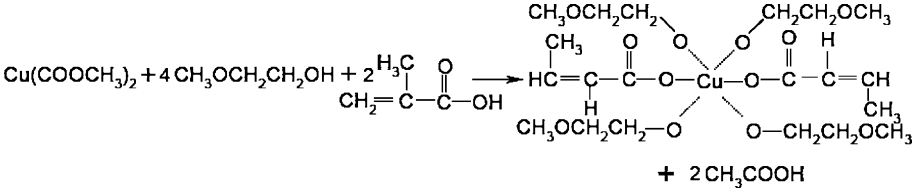

(3-3)

In the Ba-OR solution, lactic acid is employed as reactant. The lactic acid can lose a proton, when mixed with water or other organic solvent, such as OREH. Thus the lactic ligands can react with Ba^{2+} ions, producing the HOAc. The reaction can be expressed by formula (3-4).

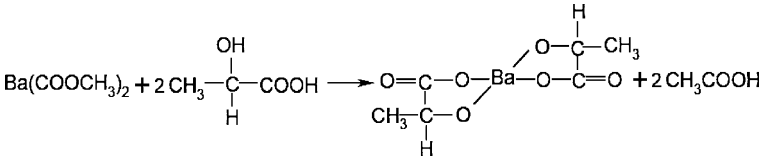

(3-4)

Therefore, the resulted YBCO precursor solution should contain at least three kinds of complexes mentioned above, and more probably, these three complexes will inter-react each other to form more complex organic groups. Due to the complexation between

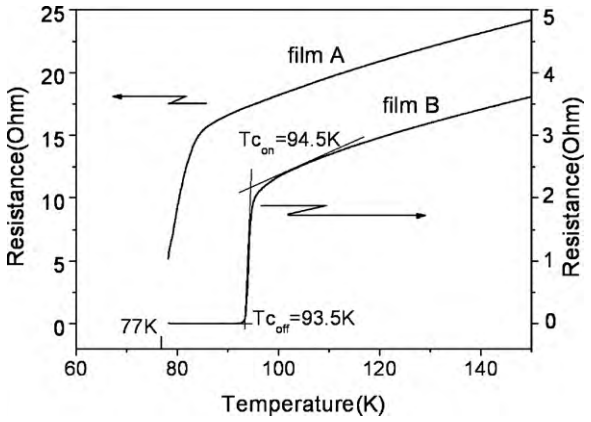

Fig. 1. *R–T* curves of YBCO films heat treated using (a) pyrolysis–annealing process (sample A) and (b) direct annealing process (sample B).

the organic groups and metallic ions, this fluorine-free YBCO solution is stable with a shelf-life of more than 1 year.

3.2. Effect of heat treatment process on phase formation

The YBCO superconductivity is sensitive to the heat treatment atmosphere. In our previous work, a series of films are prepared using different heat treatment profiles. Results indicate that the films annealed in dry air or in dry oxygen atmosphere show non-superconductivity at 77 K. Thus, annealing in humidified atmosphere, which has been used in our low-fluorine routes [11], is adopted.

The traditional heat treatment process in sol–gel preparation of oxide film involves two-steps: pyrolysis and annealing. However, our films prepared using the two-step process (the pyrolysis–annealing process) show poor-superconductivity, and more often exhibit non-superconductivity at 77 K. On the contrary, the films prepared using the direct annealing process show so good superconductivity as that derived from fluorinated routes. A dependence of resistance on temperature (*R–T* curve) is shown in Fig. 1. It can be seen from Fig. 1 that non-superconductivity at 77 K is observed for the film heat treated through pyrolysis–annealing process (film A, for example), while the film prepared using the direct annealing process (film B, for example) shows high superconductivity, with a high critical transition temperature Tc_{on} of about 94.5 K, and a sharp transition width ΔT of about 1.0 K.

To make clear the processing–structure–property relationship, X-ray diffractions were performed on films to detect their phases.

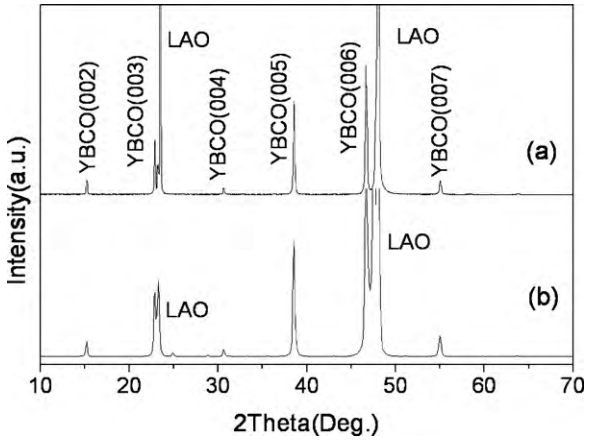

Fig. 2. X-ray theta–2theta scans of YBCO films heat treated using (a) pyrolysis–annealing process (film A) and (b) direct annealing process (film B).

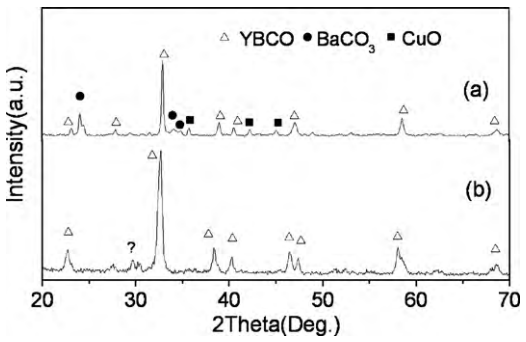

Fig. 3. Low-angle X-ray diffraction of samples heat treated using (a) pyrolysis–annealing process (film A) and (b) direct annealing process (film B).

Fig. 2 shows the XRD theta–2theta scans for the film A and film B. As can be seen in Fig. 2, only (0 0 *l*) peaks are detected for both film A and film B, and no polycrystalline YBCO peaks are observed corresponding to (0 1 3), (1 0 3), and (2 1 3) at of 32.5°, 32.8°, and 58.2°, respectively. It can be concluded from Fig. 2 that although the films heat treated either using pyrolysis–annealing process or using a direct annealing process are *c*-oriented on LAO substrate, no information about film texture or second phases can be obtained. However, we could not exclude the existence of other phases such as $BaCO_3$ phase, whose strongest diffraction peak at about 23.8° (corresponding to the $BaCO_3$ (1 1 1) plane) may be overlapped by the LAO (0 0 1) peak.

The low-angle X-ray diffractions (the angle of incident X-ray was fixed at 1°, while the acceptor is kept rotating) have also been carried out on film A and film B. Compared with traditional theta–2theta diffraction, the film orientation could not be distinguished from the low-angle XRD pattern. Nevertheless, due to the fact that incident X-ray is almost parallel to the film surface in the low-angle X-ray diffraction measurements, the phases of even very thin films can be clearly detected. The low-angle XRD pattern of film A and film B are shown in Fig. 3. A little difference between them can be found. $BaCO_3$ and CuO phases are detected in the film A, while no other phases in addition to YBCO phase are detected for film B. Thus, we can conclude that the non-superconductivity or poor-superconductivity for films obtained using the two-step pyrolysis–annealing process is ascribed to the remained second phases.

To explore the phase evolution during heat treatment process, a series of precursor films are obtained by directly heating the gel films to a peak temperature in humidified N_2/O_2 gas, then holding for 5 min and subsequently furnace cooling down to the

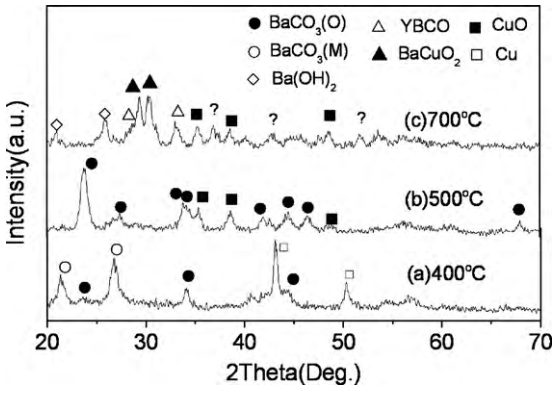

Fig. 4. XRD patterns of different films obtained by heat treatment under humidified N_2/O_2 atmosphere and quenching at a peak temperature of (a) 400 °C, (b) 500 °C and (c) 700 °C.

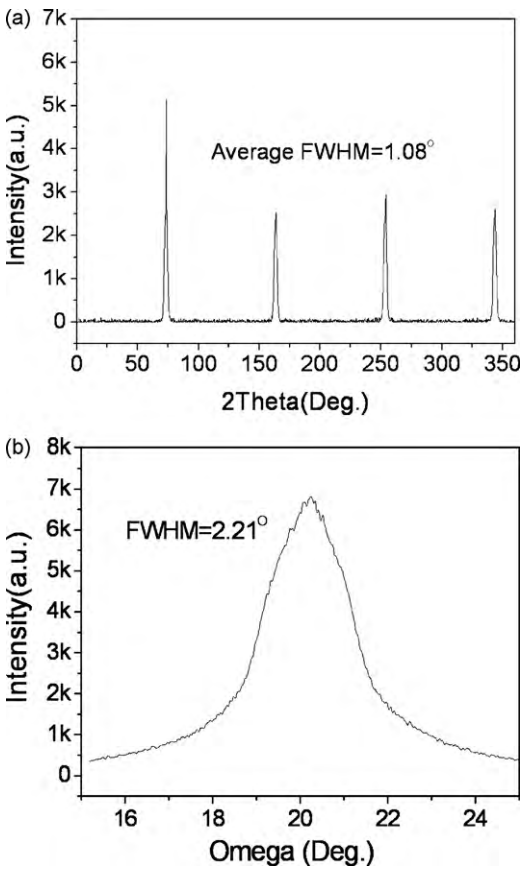

Fig. 5. XRD spectra of YBCO film B: (a) phi scan of (1 0 3) peak and (b) omega scan of (0 0 5) peak.

room temperature. Three precursor samples, which were, respectively, heated to the peak temperature of 400 °C (film-400), 500 °C (film-500) and 700 °C (film-700), are obtained. Their low-angle XRD patterns are shown in Fig. 4. Metallic Cu, monoclinic and orthorhombic $BaCO_3$ phases are detected in the film-400, as shown in Fig. 4(a). The occurrence of metallic Cu may be due to the reduced amine groups in DETA in the precursor solution and gel films, which depress the oxidization of Cu. When the temperature reaches 500 °C, the metallic Cu is oxidized into CuO, and monoclinic $BaCO_3$ is transformed to the orthorhombic $BaCO_3$ phase, as shown in Fig. 4(b). When the temperature is heated to 700 °C, $BaCO_3$ phase disappear, and $Ba(OH)_2$ phase is observed. Some other phases including YBCO, $BaCuO_2$, some unknown phases, etc., are also detected in the film-700.

As can be seen from Fig. 4, the $BaCO_3$ phase, which is even stable at the temperature of 900 °C under dry atmosphere [26], is formed during the stage of organic decomposition at 400–500 °C. However, according to Fig. 4(c), the $BaCO_3$ phase can be removed by chemical reaction with H_2O or other phases under humidified N_2/O_2 gas at the temperature above 700 °C. In the direct annealing process, the gel films are directly heated from room temperature to the temperature of YBCO phase to form at a high heating rate of 20 °C/min. The nucleation and growth of $BaCO_3$ phase should be suppressed during the rapid heating process, leading to its easy being removal at the annealing stage. Thus, phase-pure YBCO film (film B) with high superconductivity can be obtained. However, in the pyrolysis–annealing process, one or more pyrolysis processes at 400–500 °C can lead to the formation of stable $BaCO_3$ phases [26], as shown in Fig. 4(a) and (b). Thus, at the annealing stage at 780 °C, even though the formed $BaCO_3$ phases may still partially be removed by reacting with water or other phases, the driving force is be enough or a longer holding time is needed to make it completely eliminated. The obtained final YBCO film prepared by the pyrolysis–annealing process, therefore, shows poor- or even non-superconductivity due to the carbon-related groups in the YBCO lattice or between the YBCO grain-boundaries [27].

3.3. Characterization of YBCO film prepared by direct annealing process

In-plane and out-of-plane textures of YBCO films prepared using the direct annealing process, are further investigated by phi scans (φ-scans) and omega scans (ω-scans), as shown in Fig. 5. Fig. 5(a) is the φ-scan of film B. In Fig. 5(a), four peaks, 90° apart with high intensity and average full-width at half-maximum (FWHM) are obtained, indicating a good in-plane alignments in the phase-pure YBCO film. The omega scan of (0 0 5) peak of the film B, as shown in Fig. 5(b), has a FWHM of 2.21°, also indicating a good out-of-plane texture.

SEM-analysis indicates that under different heat-treating conditions, the fabricated YBCO films present varied morphologies of surface structures. The morphologies of film A and film B are, respectively, shown in Fig. 6(a) and (b). Both film A and film B have a dense microstructure almost without pores observed on the film surface. Film A has much more stripe-like *a*-axis YBCO grains on the surface compared with film B. The formation of *a*-axis grains in film A indicates the in-plane mis-orientation, which may be caused

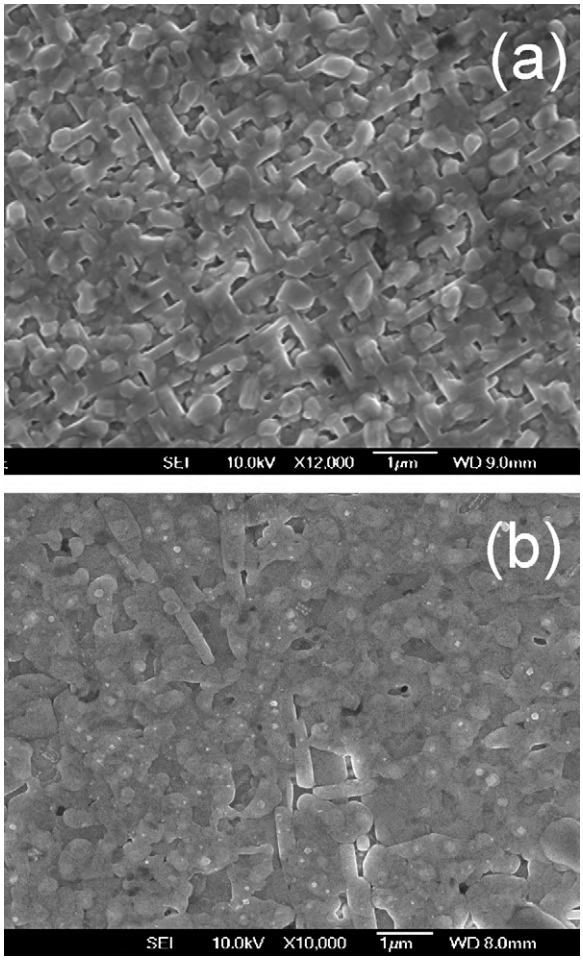

Fig. 6. SEM photograph showing the top surface of YBCO film prepared using (a) pyrolysis–annealing process and (b) direct annealing process.

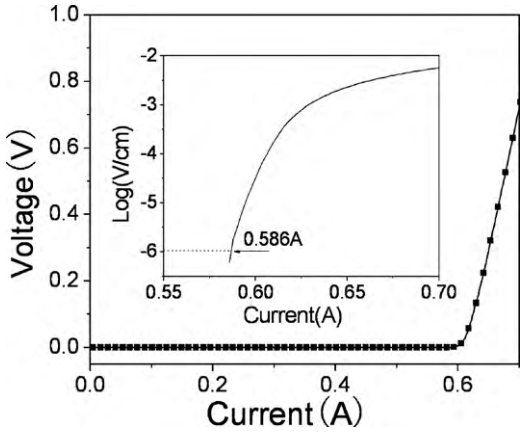

Fig. 7. *V–I* curves of YBCO film B prepared through a direct annealing process using the fluorine-free sol–gel method. The insert is a log(*E*)–*I* curve obtained after calculation according the data in the *V–I* curve.

by the second phases, and can act as blocks for superconducting current transportation.

Film B is patterned to be micro-bridge with width of 250 μm, length of 2 mm and thickness of about 230 nm. Fig. 7 shows the transport voltage–current curve (*V–I* curve) of YBCO film B. The insert is a log(*E*)–*I* curve after calculation according the data in the *V–I* curve. As can be seen from the insert, the critical current of the micro-bridge of film B is 0.586 A with a criterion of 1 μV/cm, which corresponds to the critical current density Jc of 1.02 MA/cm^2 (77 K, 0 T). High Jc of film B is attributed to its good in-plane and out-of-plane texture, dense microstructure with good inter-granular connectivity, and its phase-pure nature.

4. Conclusions

With diethylenetriamine, lactic acid, and α-methacrylic acid as complexing agents, we successfully resolved the difficulty of the low solubility of yttrium, barium and copper acetates in organic solvents by complexation method. Thus, stable fluorine-free YBCO precursor solution is prepared using the acetates as starting materials. Using the fluorine-free sol, YBCO gel films are obtained through sol–gel dip-coating method. Effects of heat treatment processes on the final film properties are examined. Results indicate that, either under a dry or a humidified atmosphere, it is difficult to obtain high-performance YBCO films by a traditional pyrolysis–annealing process, due to the formation of stable $BaCO_3$ phase during the pyrolysis process. On the other hand, high-performance YBCO superconducting films can be obtained using the fluorine-free YBCO sol by a direct annealing process without pyrolysis. The as-prepared phase-pure superconducting YBCO films have dense morphology, good in-plane and out-of-plane textures, high Tc (>94 K) and Jc (>10^6 A/cm^2).

Acknowledgements

This Research Project is supported by the National Natural Science Foundation of China (No. 50772088) and the Shaanxi Natural Science Foundation (No. 2009JQ6001).

References

[1] T. Araki, T. Yuasa, H. Kurosaki, Y. Yamada, I. Hirabayashi, T. Kato, T. Hirayama, Y. Iijima, T. Saito, Supercond. Sci. Technol. 15 (2002) L1.
[2] T. Izumi, M. Yoshizumi, J. Matsuda, K. Nakaoka, Y. Kitoh, Y. Sutoh, T. Nakanishi, A. Nakai, K. Suzuki, Y. Yamada, A. Yajima, T. Saitoh, Y. Shiohara, Physica C 463–465 (2007) 510.
[3] J.-K. Chung, W.-J. Kim, S.G. Lee, C.J. Kim, J. Alloys Compd. 449 (2008) 180.
[4] Z.M. Yu, P. Odier, L. Ortega, P.X. Zhang, C.S. Li, X.H. Liu, L. Zhou, J. Alloys Compd. 460 (2008) 519.
[5] K. Zalamova, A. Pomar, A. Palau, T. Puig, X. Obradors, Supercond. Sci. Technol. 23 (2010) 014012.
[6] L. Arda, S. Ataoglu, J. Alloys Compd. 471 (2009) 282.
[7] M.W. Rupich, X. Li, C. Thieme, S. Sathyamurthy, S. Fleshler, D. Tucker, E. Thompson, J. Schreiber, J. Lynch, D. Buczek, K. DeMoranville, Ja. Inch, P. Cedrone, J. Slack, Supercond. Sci. Technol. 23 (2010) 014015.
[8] P.C. McIntyre, M.J. Cima, M.F. Ng, J. Appl. Phys. 682 (1990) 4183.
[9] Y. Xu, A. Goyal, K. Leonard, L. Heatherly, P. Martin, IEEE Trans. Appl. Supercond. 15 (2005) 2617.
[10] H. Fuji, T. Honjo, R. Teranishi, Y. Tokunaga, J. Matsuda, S. Asada, Y. Yamada, T. Izumi, Y. Shiohara, Y. Iijima, S. Yasuhiro, K. Takashi, M. Atsushi, K. Murata, Physica C 412 (2004) 916.
[11] Y. Chen, G. Zhao, L. Lei, X. Liu, Supercond. Sci. Technol. 20 (2007) 251.
[12] D. Shi, L. Wang, J.H. Kim, X. Zhu, M. Liu, Q. Li, R. Zeng, J. Ahn, S.X. Dou, J. Yoo, Y.K. Kim, T. Yamashita, J. Barry, R. Taylor, IEEE Trans. Appl. Supercond. 19 (2009) 3208.
[13] R. Teranishi, Y. Miyanaga, K. Yamada, N. Mori, M. Mukaida, M. Miura, M. Yoshizumi, T. Izumi, M. Namba, S. Awaji, K. Watanabe, Physica C (2010), doi:10.1016/j.physc.2010.05.085.
[14] T. Manabe, M. Sohma, I. Yamaguchi, W. Kondo, K. Tsukada, S. Mizuta, T. Kumagai, Physica C 412–414 (2004) 896.
[15] N.J. Lee, T. Doi, Y. Hakuraku, N. Kashima, S. Nagaya, Physica C 412–414 (2004) 900.
[16] J. Lian, H. Yao, D. Shi, L. Wang, Y. Xu, Q. Liu, Z. Han, Supercond. Sci. Technol. 16 (2003) 838.
[17] Y. Xu, A. Goyal, J. Lian, N.A. Rutter, D. Shi, S. Sathyamurthy, M. Paranthaman, L. Wang, P.M. Martin, D.M. Kroeger, J. Am. Ceram. Soc. 87 (2008) 1669.
[18] Y. Xu, A. Goyal, K.J. Leonard, E.D. Specht, J. Am. Ceram. Soc. 89 (2006) 914.
[19] W. Cui, P. Mikheenko, L.M. Yu, T.W. Button, J.S. Abell, A. Crisan, J. Supercond. Nov. Magn. 22 (2009) 811.
[20] Y.-K. Kim, J. Yoo, K. Chung, J. Ko, Physica C 445–448 (2006) 574.
[21] Y.R. Patta, D.E. Wesolowski, M.J. Cima, Physica C 469 (2009) 129.
[22] D.E. Wesolowski, Y.R. Patta, M.J. Cima, Physica C 469 (2009) 766.
[23] G. Li, M.H. Pu, R.P. Sun, W.T. Wang, W. Wu, X. Zhang, Y. Yang, C.H. Cheng, Y. Zhao, J. Alloys Compd. 466 (2008) 429.
[24] W. Wang, J. Yang, Z. Ding, J. Non-Cryst. Solids 169 (1994) 177.
[25] J. Yang, W. Weng, Z. Ding, J. Sol–Gel. Sci. Technol. 4 (1995) 187.
[26] T. Manabe, W. Kondo, S. Mizuta, T. Kumagai, Jpn. J Appl. Phys. 30 (1991) 1000.
[27] F. Parmigiani, G. Chiarello, N. Ripamonti, H. Goretzki, U. Roll, Phys. Rev. B 36 (1987) 7148.